

Electromagnetic Interaction Between the Component Coils of Multiplex Magnets

Quyen V. M. Nguyen, Lynette Torres, and Doan N. Nguyen 

Abstract—Ultra-high field the pulsed magnets are usually designed as a group of nested, concentric coils driven by separated power sources to reduce the required driving voltages and to distribute the mechanical load. Since the magnet operates in a fast transient mode, there will be strong and complicated electromagnetic couplings between the component coils. The high eddy currents generated in the reinforcement shells of the component coils during the pulses also strongly affect these couplings. Therefore, understanding the electromagnetic interaction between the component coils will allow safer, more optimized design and operation of our magnets. This paper will focus on our finite element modeling and experimental results for the electromagnetic interactions between the component coils of the 100-T nondestructive magnet and 80-T duplex magnet at our facility.

Index Terms—Pulsed field magnet, duplex magnet, electromagnetic interaction, induced voltage, eddy current.

I. INTRODUCTION

THE very high magnetic field is an important tools for scientific research in a wide range of interesting physics phenomena such as high temperature superconductivity, topological insulators, quantum matter, and electronic structure determination [1]–[3]. Multi-shot high-field pulsed magnets allow researchers repeatedly accessing to magnetic fields up to 100 T, significantly higher than available steady-state magnetic fields of 45 T [3]–[5].

Ultra-high pulsed magnets typically have modular designs composed of several coil groups (CG) powered by separated power supplies to reduce the driven voltages and to distribute mechanical load to a larger volume [6]–[12]. Since the coil groups are driven by different circuits, it is important to understand the electromagnetic interaction between the coil groups to optimize the timing for energizing each coil group. A rare control failure may causes the magnet to be energized with one or

Manuscript received August 27, 2017; accepted November 16, 2017. Date of publication December 4, 2017; date of current version January 15, 2018. This work was undertaken at Pulsed Field Facility (PFF), NHMFL, Los Alamos National Laboratory. PFF was supported in part by NSF under Grant DMR-1157490, and in part by DOE. This work was supported by NSF under Grant DMR-1157490. The work of Q. V. M. Nguyen work was supported by NHMFL's REU program. (*Corresponding author: Doan N. Nguyen.*)

Q. V. M. Nguyen is with the Department of Aerospace Engineering, University of Texas at Austin, Austin, TX 78705 USA.

L. Torres is with the Department of Mechanical Engineering, University of New Mexico, Albuquerque, NM 87131 USA.

D. N. Nguyen is with the Pulsed Field Facility (NHMFL), Los Alamos National Laboratory, Los Alamos, NM 87545 USA (e-mail: doan@lanl.gov).

Color versions of one or more of the figures in this paper are available online at <http://ieeexplore.ieee.org>.

Digital Object Identifier 10.1109/TASC.2017.2779793

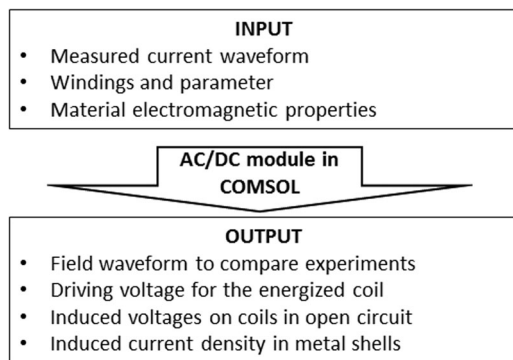


Fig. 1. Illustration of the simulation approach used to study the electromagnetic coupling between the sub-coils in our multi-plex magnets.

more coils, while other coils are in open circuit. This is known as misfired situation which may lead to high induced voltages generated on the terminals of open coil groups and therefore possible damage to the control switches or electronic/electrical components of that coil group. In many cases, windings of magnet coils are reinforced with high-strength metal shells such as stainless steel 301 or Nitronic-40 [13]–[16]. The eddy current generated in those reinforcement metal shells due to the transient of magnetic fields will strongly impact the coupling between the circuits.

In this paper, validated finite element method (FEM) simulations implemented in COMSOL Multiphysics package will be used to understand the electromagnetic coupling between the sub-coils in our 100-T and newly developed 80-T duplex magnets, as well as the role of metal reinforcement shells in reduction of the electromagnetic coupling. Fig. 1 summarizes the simulation approach for this study. Generally, the simulations will provide the waveform of the magnetic field, the waveform for driving voltage of the energized coils and the induced voltages in misfired coil groups, and the eddy current distribution in metal shells. The magnetic field waveform will be compared to the experimental data to confirm the validity of the simulations.

II. ELECTROMAGNETIC COUPLING IN THE 100-T MAGNET

Fig. 2 illustrates the structure and circuit diagram for our 100-T magnets. The magnet composes of an insert powered by 18-kV capacitor bank (cap-bank) and an outsert magnet powered by 1.4-GW generator [15], [16]. The outsert section is divided into three coil groups powered by three different power supplies. As shown in the figure, the insert consists of 8 winding layers; and each of them is reinforced by a MP35N metal layer

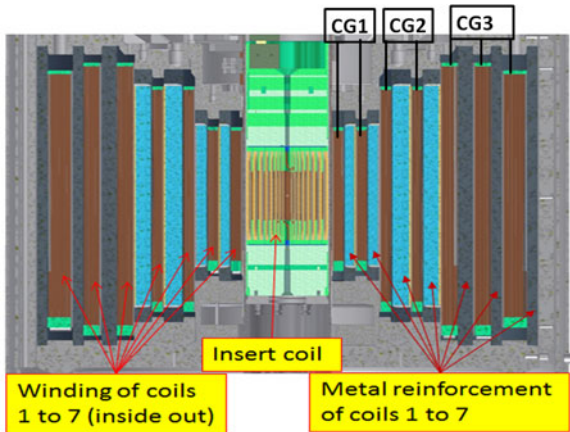


Fig. 2. 2D illustration of the structure design and circuit diagram of 100-T multi-shot magnets.

[15]. Conductor winding layers in each of the 7 coils of the outsert sections will also be reinforced by Ni-40 or stainless steel 301 shells [15], [16]. The insert of our 100-T magnets provide maximum magnetic field of about 60 T (in background field of about 40 T generated by the outsert coils) with the rise time of about 4.9 ms [15]. The high dB/dt of the insert magnetic field along with the high number of turns of the outsert coil groups may result in high induced voltages at their terminals.

Firstly, the simulation model needs to be validated. The measured waveform of electrical current passing through insert coil – when it is fired with 4-kV charged cap-bank – will be used as the input for the simulation model to calculate the magnetic field waveform and compare the results with experimental data. In the simulations, the metal reinforcement shells are considered as shorted-circuit single-turn coils. To simplify the calculations, the temperatures of reinforcement materials are assumed to be unchanged during the pulse and equal to the temperatures of the shells when the magnetic field reaches the peak value. We confirmed that, this assumption slightly overestimates the maximum induced voltages in outsert coils. This is understandable because of two reasons: (1) dependence of electrical conductivity of reinforcement metal materials on temperature is quite weak and (2) the temperature changes in metal shells around their temperatures at the peak field is considerable small.

Fig. 3 shows field waveform obtained from simulations and experiments when the insert coil is energized by 4-kV charged cap-bank. To understand the impact of the shells, simulations were performed with and without the presence of the metal shells. It is clear that the simulated results for the case with presence of metal shells reproduce very well the experimental data. On the other hand, without taking the shells into account, there is a considerable discrepancy between the simulation and experiment. This implies that with high dB/dt of the insert, the induced currents in metal shells play an important role in the electromagnetic performance of the magnets.

After being validated, simulation models were used to calculate the induced voltages generated on the coil groups of the outsert magnet when they are in open circuits. Fig. 4 plots calculated waveforms of those induced voltages and the driving

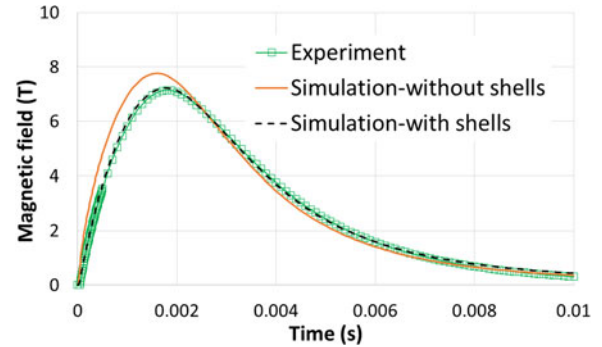


Fig. 3. Comparison of experimental and computational waveforms of magnetic field when insert coil is fired at 4 kV. Simulation results for both cases, with and without presence of metal reinforcement shells are plotted.

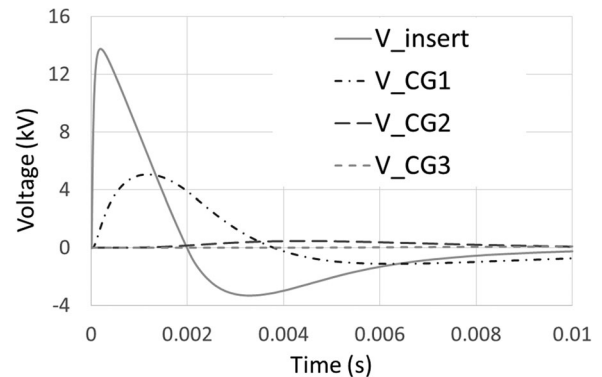


Fig. 4. Waveform of driving voltage of the insert coil and induced voltages on outsert coils when only the insert coil is energized with 15-kV bank. Metal shells are taken into account.

voltage for the insert coil when the insert coil was energized by 15 kV which is used in regular operation to provide magnetic field ~ 95 T for users. Due to eddy current in metal shells, the induced voltages reach the peak values at different times, compared to the driving voltage in the insert coil. The highest induced voltage generated on coil group 1 (CG1) with peak value is about 5 kV, which is considered in safe margin for switch and control circuit designed for outsert magnet operation. The induced voltages on CG2 and CG3 are considerably lower as expected due to stronger shielding effect provided by more metal shells placed between the insert and these coils.

To further understand the role of the metal reinforcement shells on the electromagnetic coupling between the insert and outsert coils, the induced voltage in outsert coil groups for the case without presence of metal shells were also calculated and plotted in Fig. 5. The induced voltages now have the same phase as the driving voltage of the insert, but at much larger amplitudes. As seen in Fig. 4, the outermost coil group (CG3) is nearly completely shielded by metal shells and the induced voltage on CG3 is very low. However, without the shells, the induced voltage on CG3 is very high, reaching nearly 24 kV due to its large size and number of turns.

Fig. 6 shows the distribution of eddy current in metal shells at $t = 1.5$ ms when the induced voltage in CG1 is the highest (the insert coil is energized with 15-kV charged cap-bank). In general, the induced current density is highest in the SS301 stinger

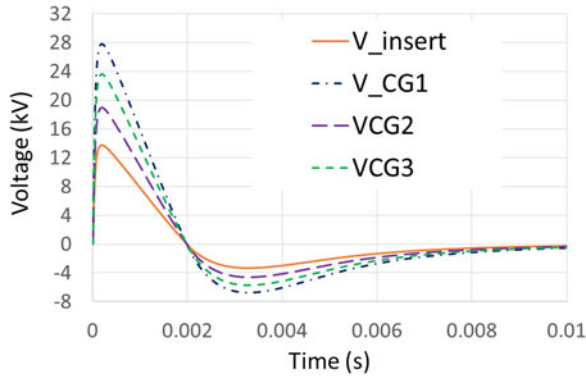


Fig. 5. Waveform of driving voltage of the insert coil and induced voltages on outsert coils when only the insert coil is energized with 15-kV-bank. In this case, metal shells are not taken into account.

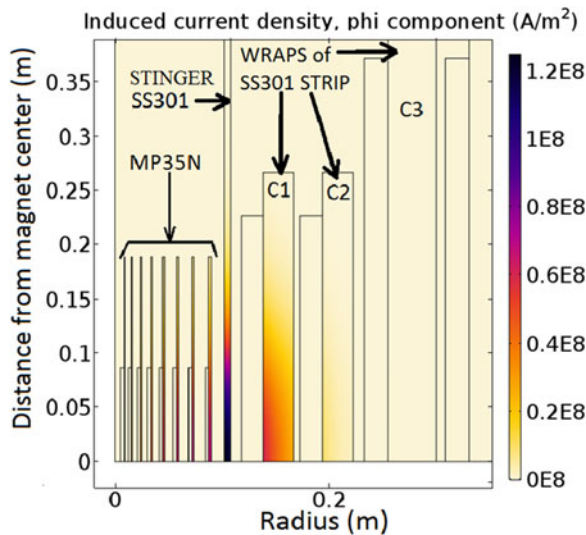


Fig. 6. Distribution of eddy current in metal shells at $t = 1.5$ ms when the induced voltage in CG1 is highest. (The insert coil is energized with 15-kV cap-bank.).

support of the insert and in wraps of SS301 thin strip utilized to reinforce coil 1 winding. The induced current densities are lower for outer shells, and very low for shells of coil 3 and beyond.

III. THE ELECTROMAGNETIC COUPLING IN 80-T DUPLEX MAGNET

The 80-T duplex magnet was recently built at LANL-PFF. Fig. 7 (Left) depicts 2D illustration for the design and current leads of our 80-T duplex magnet. Fig. 7 (Right) is the waveform of the 80-T magnetic field with individual contributions from inner coil (coil A) and outer coil (coil B). The magnets consist of two nested coils, each composes of 8 winding layers. At the highest field of 80 T, coil A is powered by 13.5-kV, 0.72-MJ cap-bank, and the outer coil B is powered by 14-kV, 2.65-MJ cap-bank. More details about the mechanical performance and field waveform of the magnet can be found at [17]. To efficiently handle the excessively high radial Lorentz forces, Zylon fiber is primarily used for reinforcement in this magnet. There are

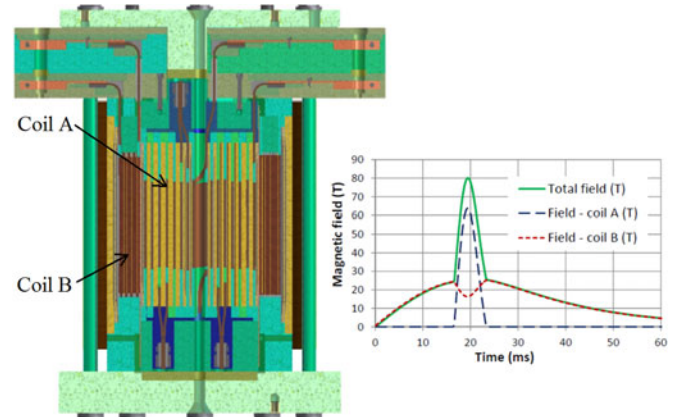


Fig. 7. (Left) 2D illustration for the design and current leads of 80-T duplex magnet; (Right) Waveform of the 80-T magnetic field with individual contributions from coils A and B.

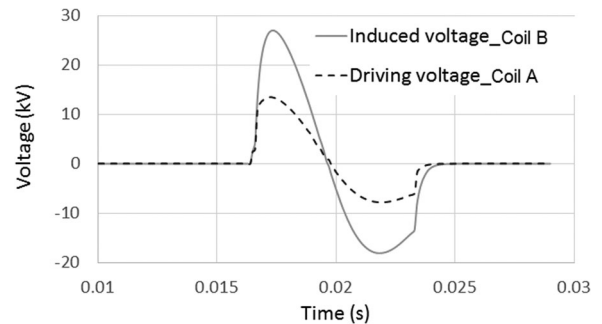


Fig. 8. Waveforms of driving voltage for coil A and induced voltage in coil B of the duplex when coil A is energized with 13.5 kV charged cap-bank.

only four metal shells composed as wraps of MP35N thin strips were used for different purposes. MP35N reinforcements used in winding layers 1 and 2 of coil A are to enhance the axial strength of these winding layers with small winding radii and to protect the experimental probe and samples in case the magnet fails at outer winding layers. The MP35N layer at the winding layer 8 of the insert is to contain the failure within coil A and prevent it to transfer to the coil B causing a higher energy failure in the outer coil. Finally, one more MP35N layer outside of the coil B is to reduce the impact of magnet failure to the surrounding equipment and structure.

The simulations were used to estimate the induced voltages on the coil A (or coil B) when it is in open circuit and the other coil is energized. Fig. 8 plots the induced voltage in coil B and the driving voltage on coil A when it is energized with 13.5 kV. Comparing to the driving voltage of coil A, the induced voltage in the outsert coil is nearly in phase but more than two times higher in amplitude. This implies that, with low conductivity and thin thickness, layers of MP35N reinforcement have weak shielding effect and do not impact much on the electromagnetic coupling between the inner and outer coils of the duplex magnet. Since the switches and control circuits of duplex coils are designed to handle voltage up to 16 kV, this study suggests that these components require additional circuit to protect them from overloaded voltage in mis-fired situation. A Metal Oxide Varistor (MOV) circuit was designed to connect in parallel with

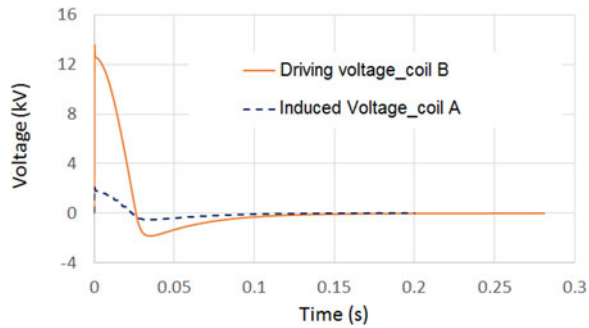


Fig. 9. Waveforms of driving voltage for coil B and induced voltage in coil A of the duplex when coil B is energized with 14 kV charged cap-bank.

coil B for this purpose. The details of this MOV circuit is over the scope of this paper and will be published elsewhere.

Fig. 9 plots the induced voltage in coil A and the driving voltage on coil B when this coil is energized with 14-kV cap-bank. In this case, the induced voltages is about 15% of the driving voltage. This implies that the mutual inductance between coil A and B is about 15% of the self-inductance of coil B. Therefore, the induced voltage on coil A due to the disturbance on coil B is expected to be always lower than the safe threshold of 16 kV and consequently, there is no need for protection MOV circuit for the inner coil.

IV. CONCLUSION REMARKS

In this paper, FEM simulations implemented in COMSOL package were used to study the electromagnetic coupling between the component coils in 100-T and 80-T magnets systems of the NHMFL-PFF at LANL. The results for 100-T magnets indicate that the eddy currents in thick metal reinforcement shells of the outer coils significantly reduce the coupling between the insert and outsert coil groups. Consequently, the induced voltages on the outsert coil groups are within the safe margin in the case that those coils are misfired for a 100-T pulse.

On the contrary, the thin MP35N reinforcement layers in duplex magnet have a weak effect on the coupling between the inner and outer coils of that magnet. As a result, in the case of the outer coil is misfired, the induced voltage on the outer coil is about twice higher than the driving voltage of the inner coil, and in the case of 80-T pulse, it is quite above the safe limit

for the switch and electronic control components. Therefore, a protection a MOV circuit connected in parallel with the outer coil is needed for safe operation of this magnet.

REFERENCES

- [1] "High magnetic field science and its application in the United States: Current status and future directions," Nat. Acad. Press, Washington, DC, USA, Rep., 2014. [Online]. Available: http://www.nap.edu/catalog.php?record_id=18355
- [2] F. Debray and P. Frings, "State of the art and developments of high field magnets at the Laboratoire National Des Champs magnétiques intenses," *Comptes Rendus Physique*, vol. 14, no. 1, pp. 2–14, Jan. 2013.
- [3] L. Li *et al.*, "Short and long pulse high magnetic field facility at the Wuhan national high magnetic field center," *IEEE Trans. Appl. Supercond.*, vol. 24, no. 3, Jun. 2014, Art. no. 9500404.
- [4] S. Zherlitsyn *et al.*, "Magnet technology development at the Dresden High Magnetic Field Laboratory," *J. Low Temp. Phys.*, vol. 170, pp. 447–451, 2013.
- [5] C. A. Swenson *et al.*, "Pulse magnet development program at NHMFL," *IEEE Trans. Appl. Supercond.*, vol. 14, no. 2, pp. 1233–1236, Mar. 2004.
- [6] J. Schillig *et al.*, "Operating experience of the United States' National High Magnetic Field Laboratory 60-T long pulse magnet," *IEEE Trans. Appl. Supercond.*, vol. 10, no. 1, pp. 526–529, Mar. 2000.
- [7] T. Peng *et al.*, "Design and performance of the first dual coil magnet at the WHMFC," *J. Low Temp. Phys.*, vol. 170, no. 5, pp. 463–468, 2013.
- [8] K. Kindo, "New pulsed-magnets for 100 T, long-pulse and diffraction measurements," *J. Phys., Conf. Ser.*, vol. 51, pp. 522–528, 2006.
- [9] T. Peng, F. Jiang, Q. Q. Sun, Y. Pan, F. Herlach, and L. Li, "Concept design of 100-T pulsed magnet at the Wuhan National High Magnetic Field Center," *IEEE Trans. Appl. Supercond.*, vol. 26, no. 4, Jun. 2016, Art. no. 4300504.
- [10] S. Zherlitsyn *et al.*, "Coil design for non-destructive pulsed-field magnets targeting 100 T," *IEEE Trans. Appl. Supercond.*, vol. 16, no. 2, pp. 1660–1663, Jun. 2006.
- [11] J. Béard *et al.*, "Special coils development at the National High Magnetic Field Laboratory in Toulouse," *J. Low Temp. Phys.*, vol. 170, pp. 442–446, 2013.
- [12] H. Ding *et al.*, "Design and analysis of power supplies for the first 100-T nondestructive magnet at the WHMFC," *IEEE Trans. Appl. Supercond.*, vol. 26, no. 4, Jun. 2016, Art. no. 4302205.
- [13] J. Bacon *et al.*, "The US-NHMFL 100 tesla multi-shot magnet," *IEEE Trans. Appl. Supercond.*, vol. 12, no. 1, pp. 695–698, Mar. 2002.
- [14] J. R. Sims *et al.*, "First 100 T nondestructive magnet," *IEEE Trans. Appl. Supercond.*, vol. 10, no. 1, pp. 510–513, Mar. 2000.
- [15] C. A. Swenson *et al.*, "Progress of the insert coil for the US-NHMFL 100 T multi-shot pulse magnet," *Physica B*, vol. 346/347, pp. 561–565, 2004.
- [16] J. R. Sims, D. G. Rickel, C. A. Swenson, J. B. Schillig, G. W. Ellis, and C. N. Ammerman, "Assembly, commissioning and operation of the NHMFL 100 tesla multi-pulse magnet system," *IEEE Trans. Appl. Supercond.*, vol. 18, no. 2, pp. 587–590, Jun. 2008.
- [17] D. N. Nguyen, "Status and Development of pulsed magnets at the NHMFL pulsed field facility," *IEEE Trans. Appl. Supercond.*, vol. 26, no. 4, Jun. 2016, Art. no. 4300905.